



# **iJRASET**

International Journal For Research in  
Applied Science and Engineering Technology



---

# **INTERNATIONAL JOURNAL FOR RESEARCH**

IN APPLIED SCIENCE & ENGINEERING TECHNOLOGY

---

**Volume: 4**

**Issue: XI**

**Month of publication: November 2016**

**DOI:**

**[www.ijraset.com](http://www.ijraset.com)**

**Call: ☎ 08813907089**

**E-mail ID: [ijraset@gmail.com](mailto:ijraset@gmail.com)**

# **A Transformerless Cascaded H-Bridge Multilevel Statcom for Power Quality Applications**

M. Satyanarayana<sup>1</sup>

Department of Electrical Engineering, UCE, Osmania University

**Abstract**— This paper is proposed a transformer less static synchronous compensator (STATCOM) system based on multi-level H-bridge converter with star configuration to compensate the reactive power in transmission system. This proposed system with controller devotes themselves not only to the current loop control but also to the dc capacitor voltage control. With regards to the current loop control, a nonlinear controller based on the passivity-based control theory is used in this cascaded structure of STATCOM. As to the dc capacitor voltage control, overall voltage control is realized by adopting a proportional integral controller. Individual balancing control is achieved by shifting the modulation wave vertically. Also fuzzy logic control controller has used instead of PI controller to have balanced DC-link Voltage. A three phase five-level H-bridge cascaded STATCOM has designed using MATLAB software for theoretical analysis. The dc capacitor voltage can be maintained at the given value effectively using the proposed control.

**Keywords**— H-bridge cascaded, proportional Integral (PI) controller, Fuzzy logic control, static synchronous compensator (STATCOM).

## **I. INTRODUCTION**

Numerous industrial applications have begun to require higher power apparatus in recent years. Some medium voltage motor drives and utility applications require medium voltage and megawatt power level. For a medium voltage grid, it is troublesome to connect only one power semiconductor switch directly. As a result, a multilevel power converter structure has been introduced as an alternative in high power and medium voltage situations. A multilevel converter not only achieves high power ratings, but also enables the use of renewable energy sources. Renewable energy sources such as photovoltaic, wind, and fuel cells can be easily interfaced to a multilevel converter system for a high power application.

The term multilevel began with the three-level converter. The term multilevel converter is utilized to refer to a power electronic circuit that could operate in an inverter or rectifier mode. Subsequently, several multilevel converter topologies have been developed. However, the elementary concept of a multilevel converter to achieve higher power is to use a series of power semiconductor switches with several lower voltage dc sources to perform the power conversion by synthesizing a *staircase voltage waveform*. Capacitors, batteries, and renewable energy voltage sources can be used as the multiple DC voltage sources. The commutation of the power switches aggregate these multiple dc sources in order to achieve high voltage at the output; however, the rated voltage of the power semiconductor switches depends only upon the rating of the dc voltage sources to which they are connected.

Flexible ac transmission systems (FACTS) are being increasingly used in power system to enhance the system utilization, power transfer capacity as well as the power quality of ac system interconnections [1], [2]. As a typical shunt FACTS device, static synchronous compensator (STATCOM) is utilized at the point of common connection (PCC) to absorb or inject the required reactive power, through which the voltage quality of PCC is improved [3]. In recent years, many topologies have been applied to the STATCOM. Among these different types of topology, H-bridge cascaded STATCOM has been widely accepted in high-power applications for the following advantages: quick response speed, small volume, high efficiency, minimal interaction with the supply grid and its individual phase control ability [4]–[7]. Compared with a diode-clamped converter or flying capacitor converter, H-bridge cascaded STATCOM can obtain a high number of levels more easily and can be connected to the grid directly without the bulky transformer. This enables us to reduce cost and improve performance of H-bridge cascaded STATCOM [8].

There are two technical challenges which exist in H-bridge cascaded STATCOM to date. First, the control method for the current loop is an important factor influencing the compensation performance. However, many non ideal factors, such as the limited bandwidth of the output current loop, the time delay induced by the signal detecting circuit, and the reference command current generation process, will deteriorate the compensation effect. Second, H-bridge cascaded STATCOM is a complicated system with many H-bridge cells in each phase, so the dc capacitor voltage imbalance issue which caused by different active power losses among the cells, different switching patterns for different cells, parameter variations of active and passive components inside cells will influence the reliability of the system and even lead to the collapse of the system. Hence, lots of researches have focused on



## International Journal for Research in Applied Science & Engineering Technology (IJRASET)

### II. PROPOSED CASCADED MULTI-LEVEL STATCOM DESIGN

The Fig. 1 shows the circuit configuration of the star-configured STATCOM cascading 12 H-bridge pulse width modulation (PWM) converters in each phase and it can be expanded easily according to the requirement. By controlling the current of STATCOM directly, it can absorb or provide the required reactive current to achieve the purpose of dynamic reactive current compensation. Finally, the power quality of the grid is improved and the grid offers the active current only. The power switching devices working in ideal condition is assumed.  $u_{sa}$ ,  $u_{sb}$ , and  $u_{sc}$  are the three-phase voltage of grid.  $u_a$ ,  $u_b$ , and  $u_c$  are the three-phase voltage of STATCOM.  $i_{sa}$ ,  $i_{sb}$ , and  $i_{sc}$  are the three-phase current of grid.  $i_a$ ,  $i_b$ , and  $i_c$  are the three-phase current of STATCOM.  $i_{la}$ ,  $i_{lb}$ , and  $i_{lc}$  are the three-phase current of load.  $U_{dc}$  is the reference voltage of dc capacitor.  $C$  is the dc capacitor.  $L$  is the inductor.  $R_s$  is the starting resistor.

TABLE-I  
CIRCUIT PARAMETERS OF THE EXPERIMENTAL SYSTEM

Grid Voltage	$U_s$	10KV
Rated Reactive power	$Q$	2 MVA
AC Inductor	$L$	10mH
Starting Resistor	$R_s$	4k $\Omega$
DC-link Capacitors	$C_{dc}$	5600 $\mu$ F
DC-link reference Voltage	$V_{dc}$	600V
Number of H-Bridges	$N$	6
Carrier Frequency	$f_c$	2.4kHz

Table I summarizes the circuit parameters. The cascade number of  $N = 12$  is assigned to H-bridge cascaded STATCOM, resulting in 36 H-bridge cells in total. Every cell is equipped with nine isolated electrolytic capacitors which the capacitance is 5600  $\mu$ F. The dc side has no external circuit and no power source except for the dc capacitor and the voltage sensor. In each cluster, an ac inductor supports the difference between the sinusoidal voltage of the grid and the ac PWM voltage of STATCOM. The ac inductor also plays an important role in filtering out switch ripples caused by PWM. For selecting insulated-gate bipolar transistor (IGBT), considering the complexities of practical industrial fields, there might be the problems of the spike current and over load. Consequently, in order to ensure the stability and reliability of H-bridge cascaded STATCOM, and also improve the over load capability, the current rating of the selected IGBT should be reserved enough safety margin. In the proposed system, 1.4 times rated current operation is guaranteed, the peak current under the 1.4 times over load condition is 224 A, the additional 76 A (30– 224 A = 76 A) is the safety margin of IGBT modules. Due to the previous considerations, the voltage and current ratings of IGBT which is selected as the switching element in main circuit are 1.7 kV and 300 A.

### III. CONTROL SYSTEM DESIGN

The Fig. 2 shows a block diagram of the control algorithm for H-bridge cascaded STATCOM. The whole control algorithm mainly consists of four parts, namely, PBC, overall voltage control, clustered balancing control, and individual balancing control. The first three parts are achieved in DSP, while the last part is achieved in the FPGA.

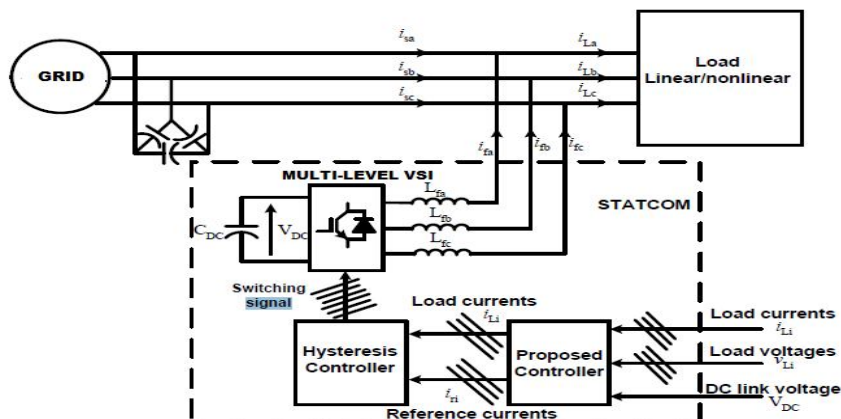


Fig.2 Schematic diagram of proposed system



## International Journal for Research in Applied Science & Engineering Technology (IJRASET)

Three-phase STATCOM is attached near to the load. The sensed DC link voltage  $V_{DC}$ , load voltages,  $V_{Li}$ , and currents,  $i_{Li}$  are manipulated via proposed controller to generate reference currents  $i_{ri}$ . Then, the Switching signals that drive the Voltage Source Inverter (VSI) are obtained from a hysteresis controller. A large DC capacitor CDC is utilized for maintaining the voltage of STATCOM DC side constant. To filter the high frequency switching ripples, a filter inductor is inserted between the STATCOM and the point of the common coupling. Occasionally, the STATCOM is coupled to the system through a transformer, which may eliminate the need for inductor filter.

The principles and fundamentals of the STATCOM are adequately highlighted in the literature [6-8]. The dynamic model of the STATCOM is well addressed in [7]; thus the focus here is on the design of the DC side capacitor and controller as given in the following sections.

### A. Dimension of the DC-link capacitor

In grid-connected wind induction generator system, the prime target of the STATCOM is partially and or fully fulfilling the generator reactive power requirements, particularly under transient conditions. Moreover, it may contribute in supplying load reactive power demands. This has the advantages of loading the transmission lines to their maximum limits. STATCOM is dimensioned in a stand-alone IG based system, according to the generator and the load reactive power requirements, considering the reactive power supplied by self excitation arrangements. In the system under consideration, 3.75kW self-excited IG is assumed to operate at 0.85 power factor (pf) lag. Thus, this generator requires around 2.4kVAR at full load conditions. It is worth to mention that the fixed excitation facilities are dimensioned for fulfilling only the generator reactive power at unity power factor full load operation at rated speed, as they supply under such conditions around 2kVAR. Thus, an additional reactive power source has to be employed for securing load requirements. Moreover, the capacitance bank excitation as mentioned suffers from the inability to cope with abrupt load change in terms of maintaining system voltage and frequency. The voltage of the DC-link voltage,  $V_{DC}$ , generally fluctuates during transient conditions in the range of (1.4-1.8) times the peak voltage of the AC voltage,  $V_{peak}$ .

The value of the DC-link CDC could be estimated from the energy balance during a disturbance, at which the STATCOM injects rated reactive power. Accordingly, the DC-link CDC is given by,

$$C_{DC} = \frac{Q_{rated\_STATCOM} nT}{V_{DCmax}^2 - V_{DCmin}^2} \quad (1)$$

where  $Q_{rated\_STATCOM}$ ,  $T$  and  $n$  are rating of STATCOM, periodic time of AC voltage cycle and ratio of response time to supply periodic time respectively.  $V_{DCmax}$  and  $V_{DCmin}$  are the maximum and minimum allowed limits of the DC voltage during a disturbance. The rated reactive power of the STATCOM,  $Q_{rated\_STATCOM}$  is 2kVAR; this value is selected according to a load of 3.5kW at 0.85pf lag, which resembles rated load of the generator. The DC-link capacitor CDC for system under concern is nearly 6mF, where the DC-link voltage  $V_{DC}$  is assumed to fluctuate between 1.8  $V_{peak}$  to 1.4  $V_{peak}$  of the AC voltage.

### B. Control Design

The control is advised based on P-Q theory. This theory is comprehensively analyzed in [20, 21]. The schematic of the proposed control technique is shown in Fig. 3. Load voltages and currents are transformed from abc to  $\alpha\beta$  coordinates; then load power are computed to defines the compensated power components. Finally, the reference currents are expressed in abc coordinates and compared with the actual currents through hysteresis band controller. A PI controller is used for regulating the DC- link voltage  $V_{DC}$ .

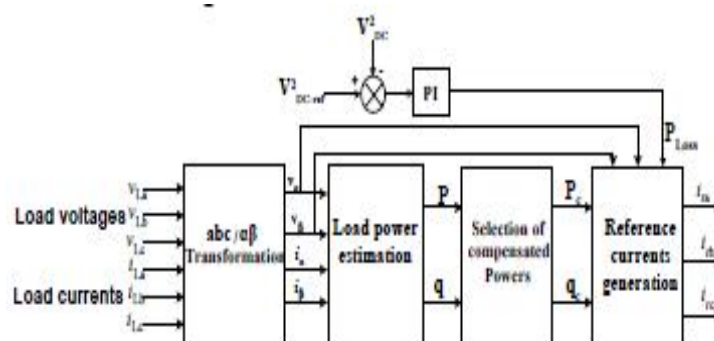


Fig-3: Proposed control scheme

## International Journal for Research in Applied Science & Engineering Technology (IJRASET)

Transforming load voltages,  $v_{La}$ ,  $v_{Lb}$  and  $v_{Lc}$ , and currents,  $i_{La}$ ,  $i_{Lb}$  and  $i_{Lc}$ , from (a-b-c) to ( $\alpha$ - $\beta$ -0) coordinates through Clarke

$$\begin{matrix} \text{formula as,} \\ \begin{bmatrix} f_{\alpha} \\ f_{\beta} \end{bmatrix} = \sqrt{\frac{2}{3}} \begin{bmatrix} 1 & -\frac{1}{2} & -\frac{1}{2} \\ 0 & \frac{\sqrt{3}}{2} & -\frac{\sqrt{3}}{2} \end{bmatrix} \begin{bmatrix} f_{La} \\ f_{Lb} \\ f_{Lc} \end{bmatrix} \end{matrix} \quad (2)$$

where  $f$  stands for voltage and current. The instantaneous active and reactive powers are given by

$$p = v_{\alpha} i_{\alpha} + v_{\beta} i_{\beta} = \bar{p} + \tilde{p} \quad (3)$$

$$q = i_{\alpha} v_{\beta} - i_{\beta} v_{\alpha} = \bar{q} + \tilde{q} \quad (4)$$

The active power  $p$  is considered to have two components: average  $\bar{p}$  and oscillating  $\tilde{p}$ . The average component  $\bar{p}$  represents the value of the instantaneous real power, which is transferred from the power supply to the load.

$\tilde{p}$  represents the oscillating energy flow per time unity, which naturally produces a zero average value; it represents an amount of additional power flow in the system without effective contribution to the energy transfer. Likewise, the load reactive power  $q$  could be separated into an average  $\bar{q}$  and oscillating  $\tilde{q}$  components.  $\bar{q}$  corresponds to the conventional three-phase reactive power, while  $\tilde{q}$  corresponds to a power that is being exchanged among the three phases, without transferring any energy between source and load. A Butterworth high pass filter is used for separating average and oscillating components of the active and reactive powers. After segregating the powers, the components need to be compensated are given by,

$$q_c^* = (k \times \bar{q} + \tilde{q}) \quad (6)$$

The gain  $k$  is used for increasing the control applicability to generator type/system layout. For, example in case of induction generator  $k$  is nearly equal to 1.0; as the STATCOM has to partially/fully satisfy the generator and load reactive power requirements in case of stand-alone mode. It is worth to mention here, that the oscillating components disappear in case of harmonic free loads; the reference currents in  $\alpha$ - $\beta$  are obtained from,

$$\begin{bmatrix} i_{\alpha}^* \\ i_{\beta}^* \end{bmatrix} = \frac{1}{v_{\alpha}^2 + v_{\beta}^2} \begin{bmatrix} v_{\alpha} & v_{\beta} \\ v_{\beta} & -v_{\alpha} \end{bmatrix} \begin{bmatrix} p_c^* + p_{loss} \\ q_c^* \end{bmatrix} \quad (7)$$

The component  $p_{loss}$ , equation (7), is added to account for the system losses. The reference currents could be expressed in abc coordinates by,

$$\begin{bmatrix} i_{ca}^* \\ i_{cb}^* \\ i_{cc}^* \end{bmatrix} = \sqrt{\frac{2}{3}} \begin{bmatrix} 1 & 0 \\ -\frac{1}{2} & \frac{\sqrt{3}}{2} \\ -\frac{1}{2} & -\frac{\sqrt{3}}{2} \end{bmatrix} \begin{bmatrix} i_{\alpha}^* \\ i_{\beta}^* \end{bmatrix} \quad (8)$$

### C. DC-link voltage Compensator

Commonly, a PI controller is used to suppress the fluctuation in the DC-link voltage of the STATCOM under non-constant load conditions. The error signal that drives the controller usually is obtained by comparing the reference  $V_{DC\_ref}$  and the DC voltage VDC. The response time of this scheme has the disadvantage of being slow. Thus, fast acting DC-link voltage controller is proposed. The compensator is driven by the difference between  $V_2$  DC\_ref and  $V_2$

DC. The mathematical basis for this advised control is given in the following. A certain amount of active power,  $P_{loss}$ , should be supplied to the STATCOM, to maintain the DC-link voltage VDC at the reference value,. Equating  $P_{loss}$  by DC-link power yields,

$$P_{loss} = V_{DC} I_{DC} \quad (9)$$

## International Journal for Research in Applied Science & Engineering Technology (IJRASET)

STATCOM dynamics equation is,

$$\frac{dV_{DC}}{dt} = \frac{I_{DC}}{C_{DC}} \quad (10)$$

Substituting (10) into (9),

$$P_{loss} = C_{DC} V_{DC} \frac{dV_{DC}}{dt} = \frac{C_{DC}}{2} \frac{dV_{DC}^2}{dt} \quad (11)$$

Taking  $V_{DC}^2$  as a state variable instead of  $V_{DC}$ , Substituting  $x = V_{DC}^2$ , averaging and extracting the transfer function  $G(s)$ ,  $x(s)/P_{loss}(s)$ ,

$$G(s) = \frac{2}{sC_{DC}} \quad (12)$$

### D. Fuzzy logic controller

The conventional PI controllers are fixed-gain feedback controllers. Therefore they cannot compensate the parameter variations in the process and cannot adapt changes in the environment. PI-controlled system is less responsive to real and relatively fast alterations in state and so the system will be slower to reach the set point. The fuzzy control algorithm is capable of improving the tracking performance as compared with the classical methods for both linear and nonlinear loads. Also, fuzzy logic is appropriate for nonlinear control because it does not use complex mathematical equation. The block diagram of fuzzy logic controller (FLC) is shown in Fig.4. The two FLC input variables are the error E and change of error CE. The behaviour of a FLC depends on the shape of membership functions of the rule base.

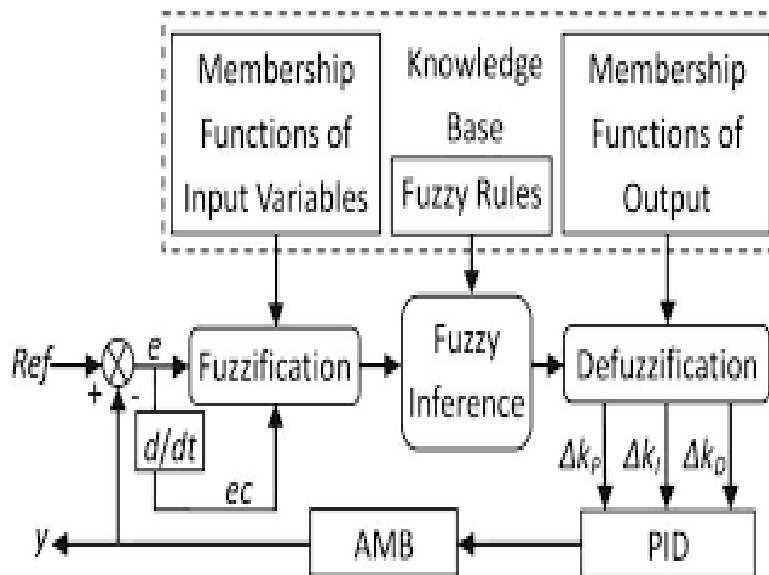


Fig.4 Block diagram of proposed Adaptive fuzzy controller

Fuzzy logic or fuzzy set theory is a new method of controlling the MPPT in obtaining the peak power point. It has the advantage of being robust, fast in response. Fuzzy controller operates in two basic modes coarse and fine modes. Input variables of fuzzy controller are error and Change of it. These variables are expressed in terms of linguistic variables or labels such as PB (positive big), PS (positive small), ZE (zero), NS (negative small) and NB (Negative big) using basic fuzzy subset. There are three stages in this control algorithm, namely fuzzification, inference method and defuzzification. An error function (E) and a change of error ( $\Delta E$ ) are created during fuzzification. These variables are then compared to a set of pre-designed values during inference method, in order to determine the appropriate response. Defuzzification is for converting the fuzzy subset of control form inference back to values. The E and  $\Delta E$  function is compared to the graph a & b to obtain a variable NB or ZE, then this parameter will be used to locate the respective output function from the fuzzy rule table.

# International Journal for Research in Applied Science & Engineering Technology (IJRASET)

Table-II

Fuzzy rule base system

$E \backslash \Delta E$	NB	NS	ZE	PS	PB
NB	ZE	ZE	NB	NB	NB
NS	ZE	ZE	NS	NS	NS
ZE	NS	ZE	ZE	ZE	PS
PS	PS	PS	PS	ZE	ZE
PB	PB	PB	PB	ZE	ZE

- 1) **Fuzzification:** Membership function's value are assigned to the linguistic variables, using seven fuzzy subsets: NB (Negative Big), NM (Negative Medium), NS (Negative small), ZE (Zero), PS (Positive small), PM (Positive Medium), and PB (Positive Big). The partition of fuzzy subsets and the shape of membership function which can adapt shape up to appropriate system. The value of error (E) and change of error ( $\Delta E$ ) are normalized by input scaling factor  $\beta_e$  and  $\beta_{de}$ . In this system input scaling has designed between  $-1$  to  $1$ . The output membership function of each rule is given by the MIN (minimum) operator, MAX (maximum) operator. The membership function of the variables error, change in error and change in reference signal for PWM generator are shown in Fig. 10(a)-(c) respectively.
- 2) **Inference engine:** Inference engine mainly consist of Fuzzy rule base and fuzzy implication sub blocks. The inputs are now fuzzified are fed to the inference engine and the rule base is then applied. The output fuzzy set are then identified using fuzzy implication method. Here we are using MIN-MAX fuzzy implication method.
- 3) **Defuzzification :** Once fuzzification is over, output fuzzy range is located. Since at this stage a non-fuzzy value of control is available a defuzzification stage is needed. Centroid defuzzification method is used for defuzzification in the proposed scheme.

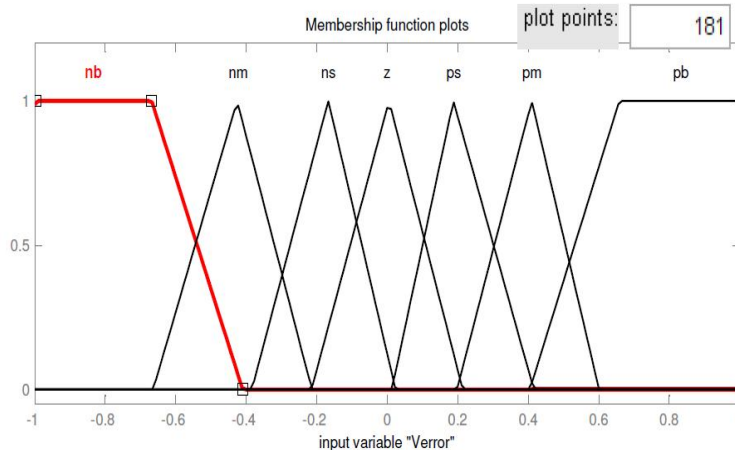


Fig. 5 (a): Membership function plots for 'e'

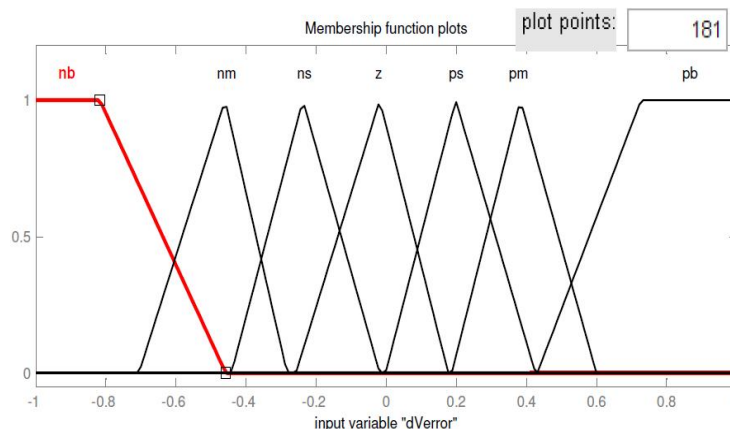


Fig.5(b): Membership function plots for ' $\Delta e$ '



## International Journal for Research in Applied Science & Engineering Technology (IJRASET)

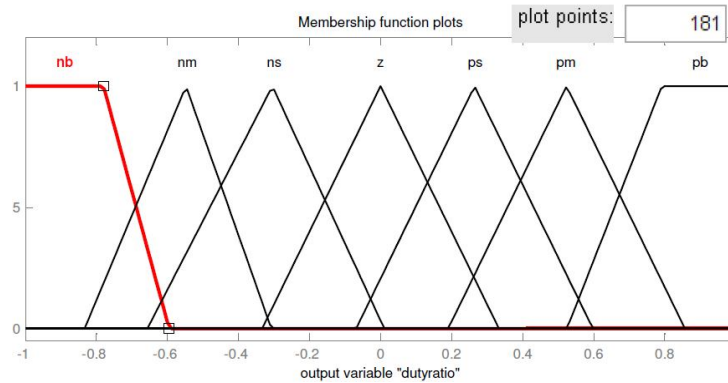


Fig. 5(c): Membership function plots for 'U'

### IV. RESULTS AND ANALYSIS

The MATLAB design of the proposed circuit is shown in fig.6. The response time of the system has drastically improved due to the introduction of closed loop control system containing different control blocks for different modes of control. Although the injection of harmonics occurs due to the introduction of power electronic equipment, it is also compensated by active disturbances rejection controller.

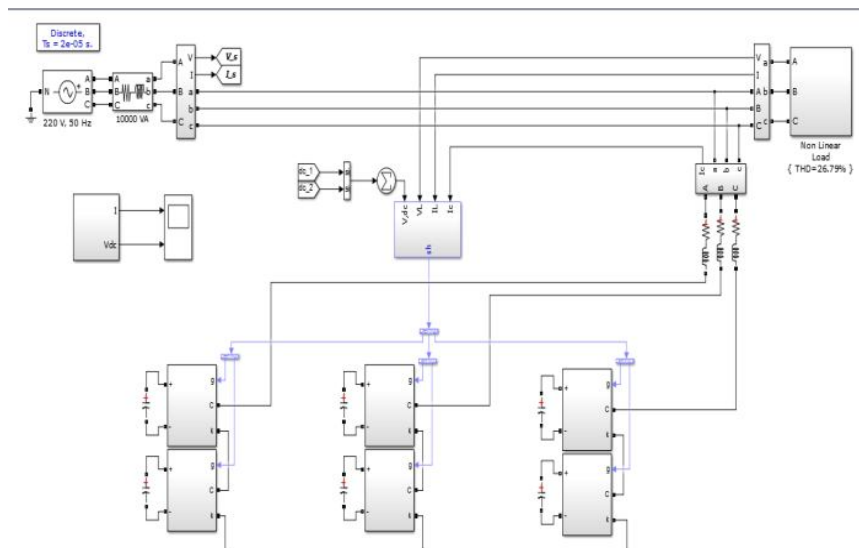


Fig.6: The MATLAB design of the proposed circuit

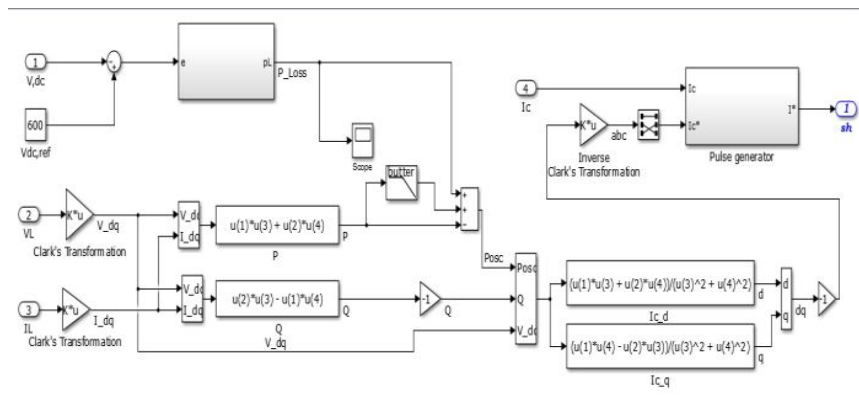


Fig.7: The proposed control strategy for multi-level STATCOM

This paper selects  $k_p = 0.05$ ,  $k_r = 10$ ,  $\omega_c = 3.14$  rad/s, and  $\omega_0 = 100\pi$  as the PR controller parameters.  $k_p = 0.5$  and  $k_i = 0.01$  are

## International Journal for Research in Applied Science & Engineering Technology (IJRASET)

selected as the PI controller parameters. The PI controller can make the voltage reach the target value rapidly, but it still requires roughly double the settling time with a much larger overshoot (greater than 6%) than that of the proposed controller.

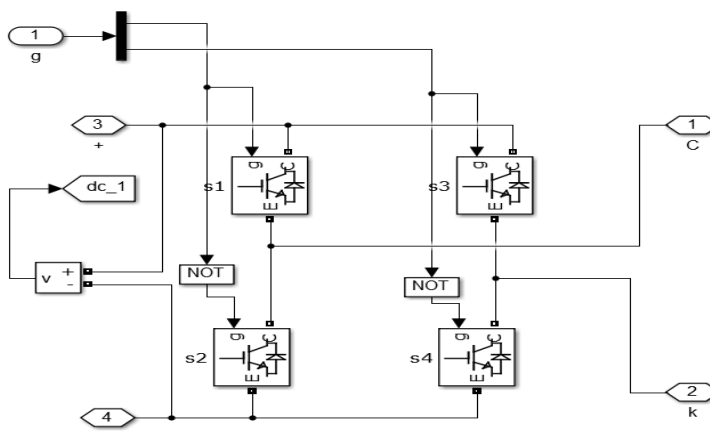


Fig.8: The H-bridge block of Cascaded multi-level Statcom

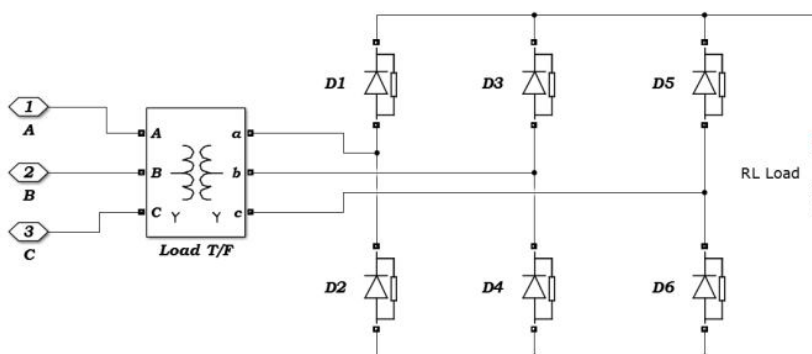


Fig.9: Non-linear load connected at the output section of the proposed system.

### A. When Using PI controller

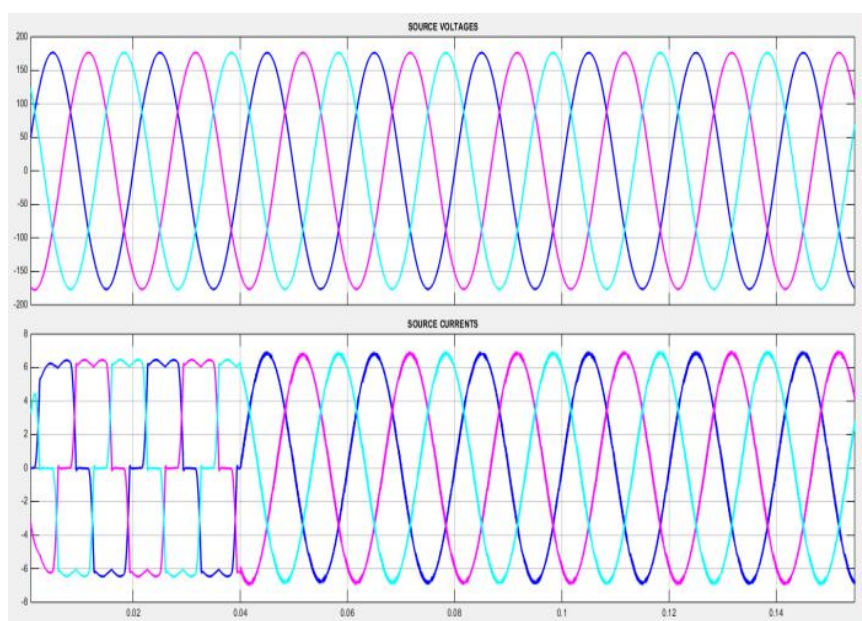


Fig.10: The input voltage and current of proposed circuit when using PI controller

## International Journal for Research in Applied Science & Engineering Technology (IJRASET)

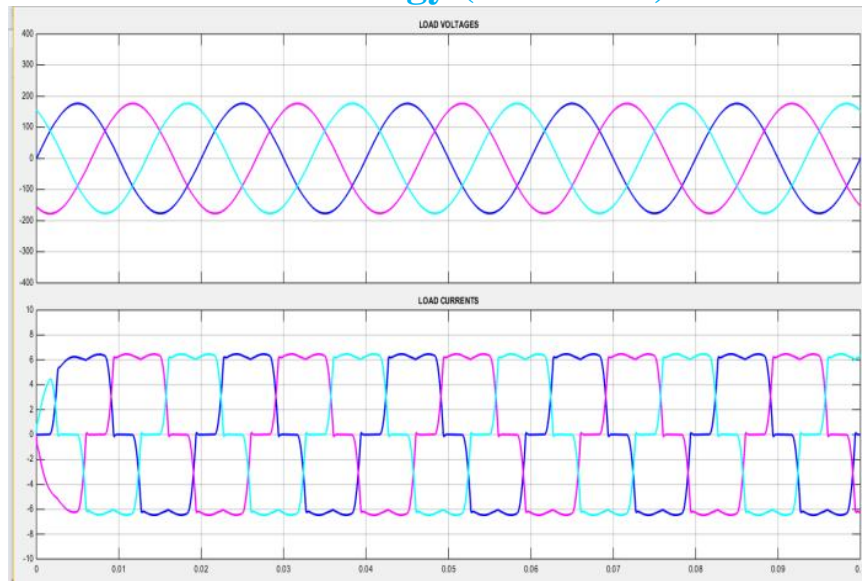


Fig.11: The load voltages and currents

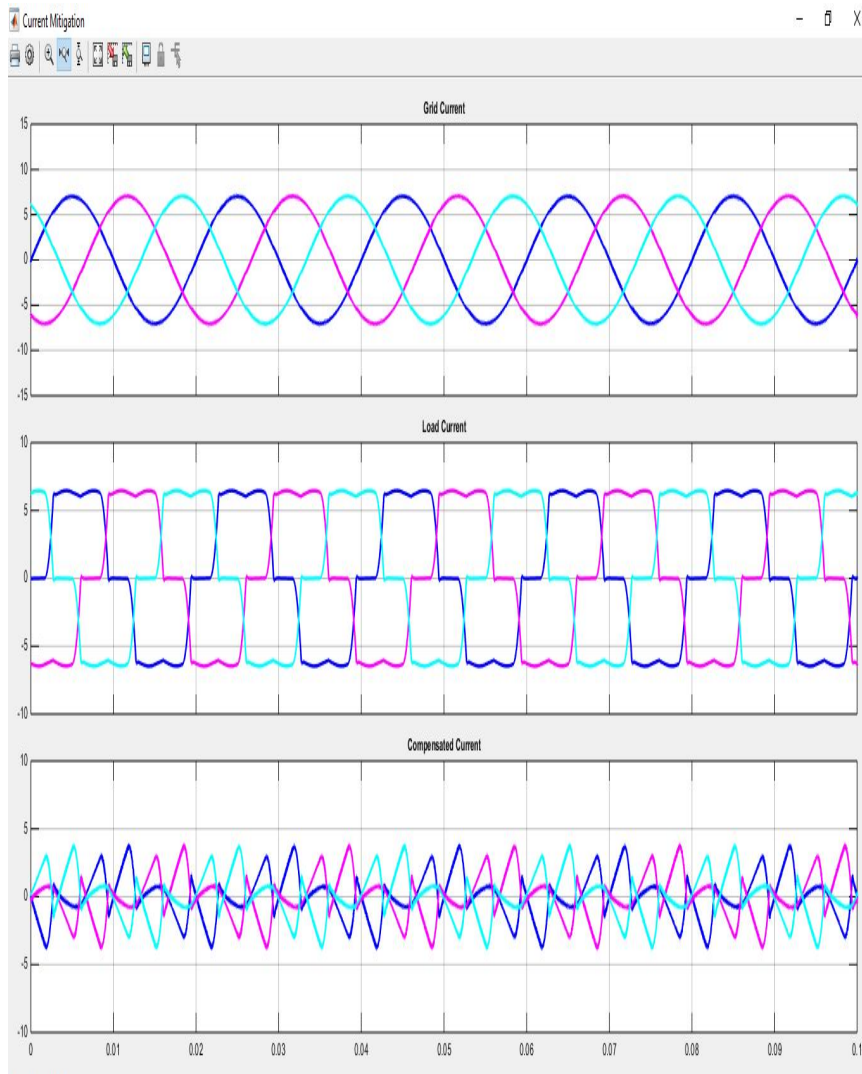


Fig.12: The grid currents, Load currents and Compensation currents

# International Journal for Research in Applied Science & Engineering Technology (IJRASET)

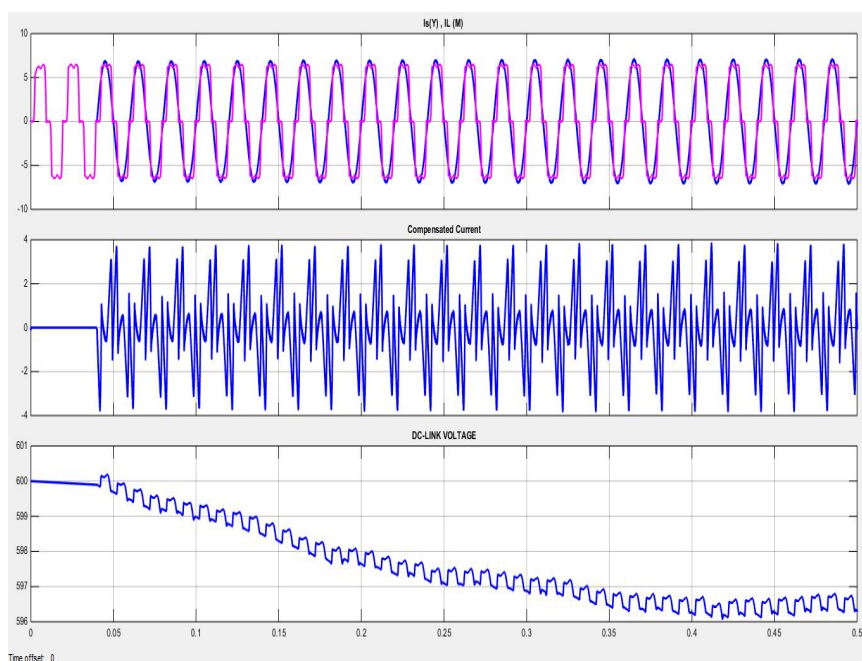


Fig.13: The line currents and load currents before and after compensation and DC-link voltage.

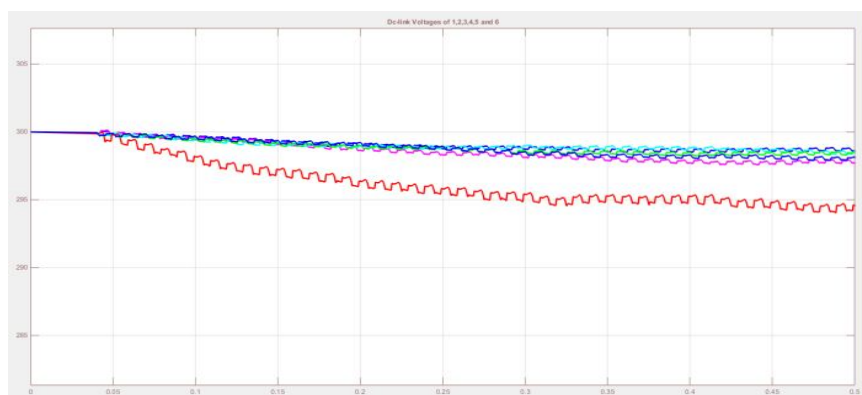


Fig.14: DC-link voltages of all six capacitors of proposed controller when using PI.

## B. With Fuzzy logic controller

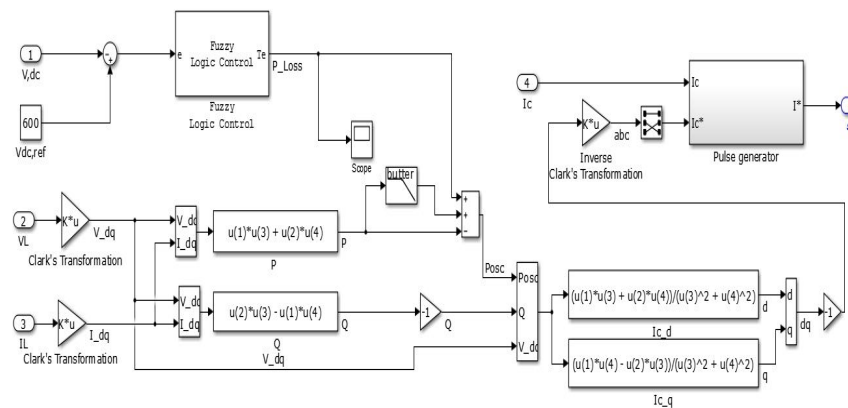


Fig.15: The proposed controller with Fuzzy logic controller instead of PI.



## International Journal for Research in Applied Science & Engineering Technology (IJRASET)



Fig.16: DC-link voltages of all six capacitors of proposed controller when using PI.

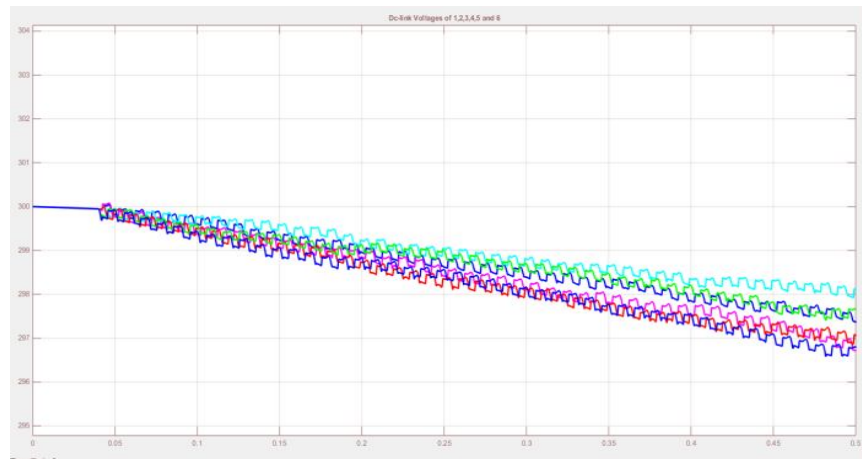


Fig.17: Zoomed view of DC-link voltages of all six capacitors of proposed controller when using Fuzzy controller. It is observed that the DC-link is unaffected when using robust Fuzzy logic controller instead of PI controller.

### V. CONCLUSIONS

This paper is proposed of STATCOM based on Cascaded H-bridge multilevel converter with star configuration. A control method has also proposed in detail based on PI and Fuzzy. The proposed methods have the following characteristics. A nonlinear controller is first used in STATCOM with this cascaded structure for the current loop control, and the viability is verified by the simulation results. The Fuzzy controller is designed for overall voltage control and the experimental result proves that it has better performance in terms of response time and damping profile compared with the PI controller. The H-bridge cascaded STATCOM for clustered balancing control and the experimental results verify that it can realize excellent dynamic compensation for the outside disturbance. The individual balancing control method which is realized by shifting the modulation wave. The simulation results have confirmed that the proposed methods are feasible and effective. In addition, the findings of this study can be extended to the control of any multilevel voltage source converter, especially those with H-bridge cascaded structure.

### REFERENCES

- [1] Gultekin and M. Ermis, "Cascaded multilevel converter-based transmission STATCOM: System design methodology and development of a 12 kV  $\pm$ 12 MVar power stage," IEEE Trans. Power Electron., vol. 28, no. 11, pp. 4930–4950, Nov. 2013.
- [2] B. Gultekin, C. O. Gercik, T. Atalik, M. Deniz, N. Bicer, M. Ermis, K. Kose, C. Ermis, E. Koc, I. C. Adirci, A. Acik, Y. Akkaya, H. Toygar, and S. Bideci, "Design and implementation of a 154-kV $\pm$ 50-Mvar transmission STATCOM based on 21-level cascaded multilevel converter," IEEE Trans. Ind. Appl., vol. 48, no. 3, pp. 1030–1045, May/Jun. 2012.
- [3] S. Kouro, M. Malinowski, K. Gopakumar, L. G. Franquelo, J. Pou, J. Rodriguez, B. Wu, M. A. Perez, and J. I. Leon, "Recent advances and industrial applications of multilevel converters," IEEE Trans. Ind. Electron., vol. 57, no. 8, pp. 2553–2580, Aug. 2010.
- [4] F. Z. Peng, J.-S. Lai, J. W. McKeever, and J. VanCoevering, "A multilevel voltage-source inverter with separate DC sources for static var generation," IEEE Trans. Ind. Appl., vol. 32, no. 5, pp. 1130–1138, Sep./Oct. 1996. [5] Y. S. Lai and F. S. Shyu, "Topology for hybrid multilevel inverter," Proc. Inst. Elect. Eng.—Elect. Power Appl., vol. 149, no. 6, pp. 449–458, Nov. 2002.
- [5] D. Soto and T. C. Green, "A comparison of high-power converter topologies for the implementation of FACTS controllers," IEEE Trans. Ind. Electron., vol. 49, no. 5, pp. 1072–1080, Oct. 2002.
- [6] C. K. Lee, J. S. K. Leung, S. Y. R. Hui, and H. S.-H. Chung, "Circuit-level comparison of STATCOM technologies," IEEE Trans. Power Electron., vol. 18, no.

## International Journal for Research in Applied Science & Engineering Technology (IJRASET)

- 4, pp. 1084–1092, Jul. 2003.
- [7] H. Akagi, S. Inoue, and T. Yoshii, “Control and performance of a transformerless cascade PWM STATCOM with star configuration,” *IEEE Trans. Ind. Appl.*, vol. 43, no. 4, pp. 1041–1049, Jul./Aug. 2007.
- [8] A. H. Norouzi and A. M. Sharaf, “Two control scheme to enhance the dynamic performance of the STATCOM and SSSC,” *IEEE Trans. Power Del.*, vol. 20, no. 1, pp. 435–442, Jan. 2005.
- [9] C. Schauder, M. Gernhardt, E. Stacey, T. Lemak, L. Gyugyi, T. W. Cease, and A. Edris, “Operation of  $\pm 100$  MVar TVA STATCOM,” *IEEE Trans. Power Del.*, vol. 12, no. 4, pp. 1805–1822, Oct. 1997.
- [10] C. H. Liu and Y. Y. Hsu, “Design of a self-tuning PI controller for a STATCOM using particle swarm optimization,” *IEEE Trans. Ind. Electron.*, vol. 57, no. 2, pp. 702–715, Feb. 2010.
- [11] S. Mohagheghi, Y. Del Valle, G. K. Venayagamoorthy, and R. G. Harley, “A proportional-integrator type adaptive critic design-based neuro controller for a static compensator in a multimachine power system,” *IEEE Trans. Ind. Electron.*, vol. 54, no. 1, pp. 86–96, Feb. 2007.
- [12] H. F. Wang, H. Li, and H. Chen, “Application of cell immune response modelling to power system voltage control by STATCOM,” *Proc. Inst. Elect. Eng. Gener. Transm. Distrib.*, vol. 149, no. 1, pp. 102–107, Jan. 2002.
- [13] A. Jain, K. Joshi, A. Behal, and N. Mohan, “Voltage regulation with STATCOMs: Modeling, control and results,” *IEEE Trans. Power Del.*, vol. 21, no. 2, pp. 726–735, Apr. 2006.
- [14] V. Spitsa, A. Alexandrovitz, and E. Zeheb, “Design of a robust state feedback controller for a STATCOM using a zero set concept,” *IEEE Trans. Power Del.*, vol. 25, no. 1, pp. 456–467, Jan. 2010.
- [15] C. D. Townsend, T. J. Summers, and R. E. Betz, “Multigoal heuristic model predictive control technique applied to a cascaded H-bridge STATCOM,” *IEEE Trans. Power Electron.*, vol. 27, no. 3, pp. 1191–1200, Mar. 2012.
- [16] C. D. Townsend, T. J. Summers, J. Vodden, A. J. Watson, R. E. Betz, and J. C. Clare, “Optimization of switching losses and capacitor voltage ripple using model predictive control of a cascaded H-bridge multilevel STATCOM,” *IEEE Trans. Power Electron.*, vol. 28, no. 7, pp. 3077–3087, Jul. 2013.



### AUTHOR DETAILS

M. Satyanarayana working as Research Assistant in the department of Electrical Engineering, University college of engineering, Osmania University, Hyderabad in the area of Multi-level Inverters. He has two years of Industrial experience on hardware development and Simulation of Power system and Power electronic integrated equipment. He solved several IEEE papers and published several journals and conference proceedings. He worked as project developer at NI-MSME, Hyderabad. He also worked as Assistant professor in Trinity engineering college, Karimnagar. He is currently working towards research in the area of Multi-level Inverters. His area of interest includes Multi-Level converters, Distribution power generation, and Power quality.



10.22214/IJRASET



45.98



IMPACT FACTOR:  
7.129



IMPACT FACTOR:  
7.429



# INTERNATIONAL JOURNAL FOR RESEARCH

IN APPLIED SCIENCE & ENGINEERING TECHNOLOGY

Call : 08813907089  (24\*7 Support on Whatsapp)